



TITLE:

Electronic behaviors of high-dose phosphorus-ion implanted 4H-SiC(0001)

AUTHOR(S):

Negoro, Y; Katsumoto, K; Kimoto, T; Matsunami, H

CITATION:

Negoro, Y ...[et al]. Electronic behaviors of high-dose phosphorus-ion implanted 4H-SiC(0001). Journal of Applied Physics 2004, 96(1): 224-228

ISSUE DATE:

2004-07-01

URL:

<http://hdl.handle.net/2433/24196>

RIGHT:

Copyright 2004 American Institute of Physics. This article may be downloaded for personal use only. Any other use requires prior permission of the author and the American Institute of Physics.

Electronic behaviors of high-dose phosphorus-ion implanted 4H-SiC (0001)

Y. Negoro,^{a)} K. Katsumoto, T. Kimoto, and H. Matsunami

Department of Electronic Science and Engineering, Kyoto University, Kyotodaigaku-katsura, Nishikyo, Kyoto 615-8510, Japan

(Received 12 January 2004; accepted 6 April 2004)

High-dose phosphorus-ion (P^+) implantation into 4H-SiC (0001) followed by high-temperature annealing has been investigated. Annealing with a graphite cap largely suppressed the surface roughening of implanted SiC. The surface stoichiometry of implanted SiC was examined by x-ray photoelectron spectroscopy. Electronic behaviors of P^+ -implanted SiC are discussed based on Hall effect measurements. There is no significant difference in the sheet resistance between SiC annealed with a graphite cap and without a graphite cap. The sheet resistance (resistivity) takes a minimum value of $45 \Omega/\square$ ($0.9 \text{ m}\Omega\text{cm}$) at an implant dose of $6.0 \times 10^{16} \text{ cm}^{-2}$. The sheet resistance shows a weak temperature dependence. © 2004 American Institute of Physics. [DOI: 10.1063/1.1756213]

I. INTRODUCTION

Silicon carbide (SiC) is an attractive material for high-power, high-temperature, and high-frequency devices because of its superior properties such as wide band gap, high breakdown field, high thermal conductivity, and high saturation electron drift velocity.¹ These properties have roots in a strong chemical bonding between silicon and carbon. However, it brings difficulties to device processing: for example, a relatively high temperature is generally required. Device process technologies in SiC are one of the crucial issues to realize high-performance SiC electronic devices. Successful selective doping can be made only by ion implantation, because the low diffusion coefficients of impurities in SiC (Ref. 2) make a diffusion process very difficult.

Ion implantation with a high donor dose into SiC is required to reduce resistivities of Ohmic contacts as well as source and drain regions in field-effect transistors (FETs). To form selective n^+ regions with a low resistivity in SiC, nitrogen ion (N^+) and phosphorus ion (P^+) implantations are commonly employed. Recently P^+ implantation has attracted increasing attention to obtain lower sheet resistances. A lower sheet resistance of $29 \Omega/\square$ ($0.8 \mu\text{m}$ -thick layer), corresponding to a resistivity of $2.3 \text{ m}\Omega\text{cm}$ (800°C implanted and 1700°C annealed) has been achieved for 4H-SiC (0001) by Schmid *et al.*,³ while the lowest resistance of N^+ -implanted SiC ever reported is $290 \Omega/\square$ (Ref. 4) ($0.5 \mu\text{m}$ -thick layer). The relatively high resistance of N^+ -implanted layers might be due to a lower solubility limit of N in SiC⁵ (about 10^{19} cm^{-3}). At this point, high-dose P^+ implantation at an elevated temperature followed by annealing at a high temperature above 1600°C is effective to reduce sheet resistances.^{5,6} The high-temperature annealing, however, causes a roughened surface of implanted SiC, which may adversely affect device performance.⁷ Several techniques to suppress the surface roughening have recently been demonstrated: Annealing with a SiH_4 overpressure,⁸ an-

nealing with an AlN cap,⁹ and rapid thermal annealing (RTA).¹⁰

In this study, electrical properties of high-dose P^+ -implanted 4H-SiC are examined together with process usability of graphite cap. After a brief description of a technique to suppress the surface roughening by using a graphite cap during high-temperature annealing, electronic behaviors of P^+ -implanted 4H-SiC are discussed based on Hall effect measurements. It is examined whether the surface roughening of P^+ -implanted samples adversely affects electrical behaviors or not. The implant-dose dependence and the temperature dependence of electrical properties are characterized.

II. EXPERIMENTS

The starting substrates are n -type 8° off-axis 4H-SiC (0001) purchased from Cree. Boron-doped p -type 4H-SiC epilayers were grown on the substrates by chemical vapor deposition (CVD) in the authors' group. The net acceptor concentration of epilayers was about $1 \times 10^{16} \text{ cm}^{-3}$. Multiple implantation of P^+ was carried out at 500°C to form a $0.2 \mu\text{m}$ -deep box profile of P atoms. The implant energies and dose ratios were 180, 120, 80, 30, 10 keV and 0.520, 0.130, 0.210, 0.108, 0.032, respectively. The total dose was varied from $1.0 \times 10^{15} \text{ cm}^{-2}$ to $6.0 \times 10^{16} \text{ cm}^{-2}$, corresponding to the phosphorus atom concentration from $5.0 \times 10^{19} \text{ cm}^{-3}$ to $3.0 \times 10^{21} \text{ cm}^{-3}$.

After ion implantation, a graphite cap was formed on the implanted SiC as follows: First, a photo-resist (AZ5218-E, Clariant Japan K. K.) was spin-coated on the whole surface of implanted SiC. The thickness of spin-coated photo-resist was about $3 \mu\text{m}$. Second, the spin-coated photo-resist was converted to graphite by thermal treatment at 750°C for 15 min in an Ar ambient. The thickness of graphite cap was about $1 \mu\text{m}$, observed by cross-sectional scanning electron microscopy (SEM). Then, postimplantation annealing was performed in a CVD reactor at 1700°C for 1 or 30 min in a pure Ar ambient. Finally, the graphite cap was successfully

^{a)}Electronic mail: negoro@semicon.kuee.kyoto-u.ac.jp

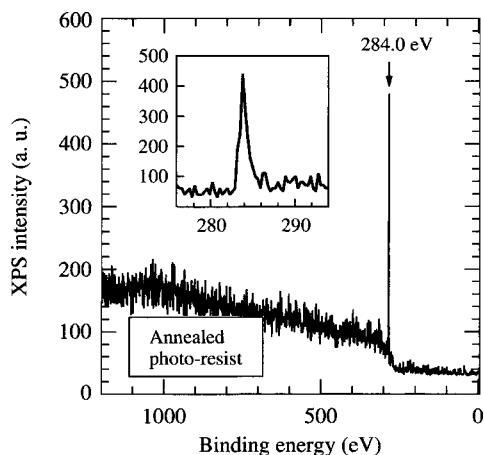


FIG. 1. XPS spectrum of graphite converted from photo-resist on 4H-SiC (0001).

removed in an O_2 ambient at 900 °C for 30 min.

The electrical properties of P^+ -implanted regions were characterized by Hall effect measurements using the van der Pauw configuration at 80–330 K. To avoid leakage current along the sample edges, clover-leaf-shaped mesa structures ($4 \times 4 \text{ mm}^2$) were prepared by reactive ion etching (RIE). Ohmic contacts in the van der Pauw arrangement were formed by evaporating Al and annealing at 500 °C for 5 min. The electrodes behave as Ohmic contacts on highly doped n -type SiC, being sufficient for Hall effect measurements.

The stoichiometry of SiC surface was examined by x-ray photoelectron spectroscopy (XPS) with an x-ray source of Al $K\alpha_1$ (1846.6 eV). Surface morphologies and XPS spectra of aluminum-ion (Al^+)-implanted layers were characterized as well as P^+ -implanted layers for a practical use of graphite cap.

III. RESULTS AND DISCUSSION

A. Composition of cap and stoichiometry of SiC surface

Figure 1 shows the XPS spectrum of annealed photo-resist on implanted SiC after postimplantation annealing at 1700 °C. A sharp peak was found at a binding energy of 284.0 eV, which can be correlated to the binding energy of C_{1s} in graphite. This indicates that the annealed photo-resist was truly converted to graphite.

The XPS spectra of SiC implanted with $3.0 \times 10^{16} \text{ cm}^{-2}$ of Al^+ after removing the graphite cap are shown in Fig. 2(a). The XPS spectra of SiC implanted with Al^+ and annealed without a graphite cap (bare-annealed SiC), and as-grown p -SiC are also shown in Figs. 2(b) and (c), respectively. It should be noted that the same oxidation process (900 °C for 30 min) was employed for bare-annealed samples to remove a very thin C-rich surface,¹¹ which is created during high-temperature annealing, prior to the XPS measurements. The purpose of XPS measurements here is to determine whether a graphite cap adversely affects the implanted SiC surface or not.

Two sharp peaks with a binding energy of 99.6 and 282.0 eV were obtained from all three samples, which can be

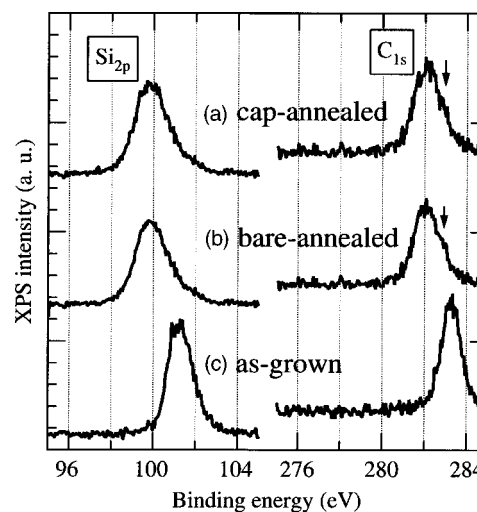


FIG. 2. XPS spectra of (a) SiC implanted and annealed with a graphite cap; (b) SiC implanted and annealed without a graphite cap; and (c) as-grown SiC.

correlated to the binding energy of Si_{2p} and C_{1s} in SiC, respectively. A shoulder is observed in Figs. 2(a) and (b) on the high-energy flank of the C_{1s} peak. Since the shoulder is observed at about 283.0 eV both in the samples annealed with a graphite cap and without a graphite cap, it may be reasonable that the shoulder is not attributed to a graphite residue from a graphite cap. A top-most C-rich layer, which may not be removed by the oxidation at 900 °C, is created by the combination of high-dose ion-implantation and high-temperature annealing, or even by high-temperature annealing only. The surface stoichiometry of implanted SiC and as-grown SiC was characterized by analyzing the XPS spectra, using the ratio of integral intensity for C_{1s} peak to that for the Si_{2p} peak. Considering the relative sensitivity of each element in XPS analysis, the surface C/Si ratio for graphite-cap-annealed SiC was 0.96. The ratio for bare-annealed SiC and as-grown SiC was 0.97 and 0.99, respectively. These results indicate that the surface stoichiometry of implanted SiC was almost maintained after high-temperature annealing with a graphite cap. No significant difference in the surface C/Si ratio was found between Al^+ -implanted and P^+ -implanted samples. Thus, a graphite cap does not adversely affect the SiC surface in this annealing process.

B. Suppression of surface roughening

Figure 3 shows the AFM images of P^+ -implanted 4H-SiC (0001) surfaces for three different doses. The upper and lower images of the figure show graphite-cap-annealed and bare-annealed samples, respectively. In the case of graphite-cap annealing, the surface of implanted SiC retained excellent flatness after high-temperature annealing. The rms surface roughness for the sample with a dose of $1.0 \times 10^{16} \text{ cm}^{-2}$ was 1.0 nm. This is about 15 times smaller than that of bare-annealed SiC. The graphite cap may have suppressed the migration of Si and C atoms on the surface of implanted SiC during high-temperature annealing, resulting in the excellent flatness without macrostep formation. Almost no difference was observed between P^+ -implanted

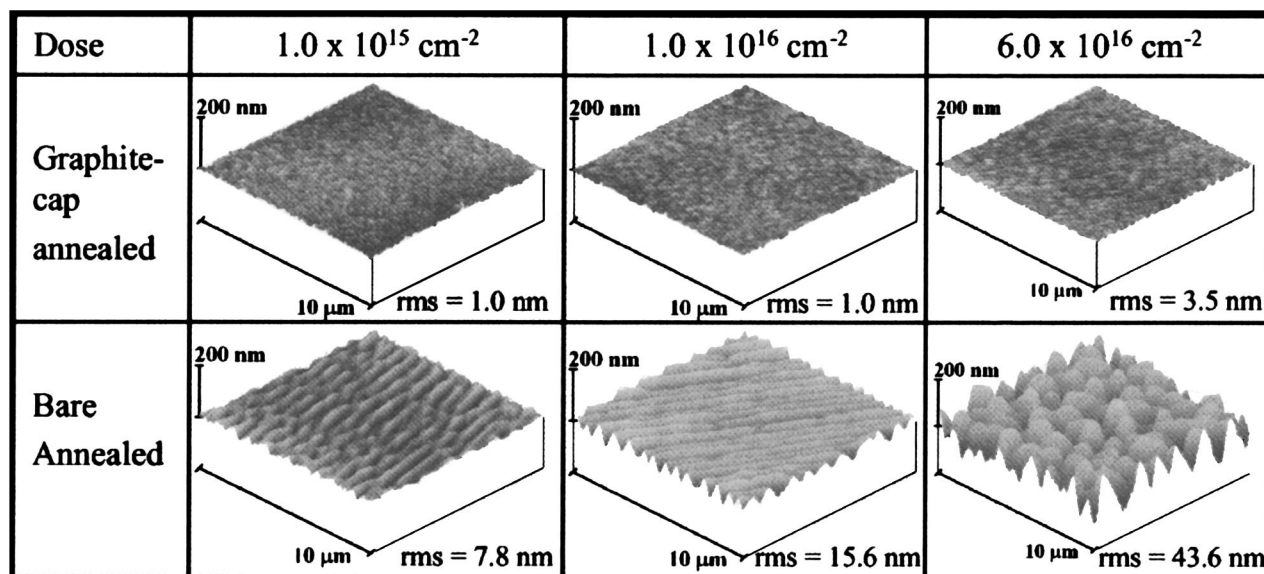


FIG. 3. AFM images of high-dose P^+ -implanted 4H-SiC (0001) after high-temperature annealing at 1700 °C for 30 min. The upper and lower sides depict samples annealed with a graphite cap and bare-annealed samples, respectively.

samples and Al^+ -implanted samples. This convenient technique suppressing the roughening is attractive for SiC device fabrication.

C. Electrical properties

Figure 4 shows the implant-dose dependence of (a) sheet resistance and (b) free-electron concentration at room temperature (RT) for P^+ -implanted 4H-SiC (0001). In Fig. 4(a), there is little difference observed in the sheet resistance between graphite-cap-annealed SiC and bare-annealed SiC. The sheet resistance is significantly reduced down to about $70 \Omega/\square$, by increasing the P^+ dose up to $4.0 \times 10^{15} \text{ cm}^{-2}$. When the implant dose changed from 4.0×10^{15} to $6.0 \times 10^{16} \text{ cm}^{-2}$, the sheet resistance decreased gradually. The sheet resistance takes the lowest value of $46 \Omega/\square$ at an implant dose of $6.0 \times 10^{16} \text{ cm}^{-2}$. The corresponding resistivity is $0.9 \text{ m}\Omega\text{cm}$, which is the lowest resistivity ever reported for any n -type SiC. Even in 1 min annealing, the sheet resistances was as low as that of 30-min-annealed samples.

In Fig. 4(b), the dashed line depicts the calculated free-electron concentration at RT, assuming that all implanted P atoms work as ionized donors at RT. For the relatively low implant dose of 1.0×10^{15} and $4.0 \times 10^{15} \text{ cm}^{-2}$, more than 50% of implanted P atoms act as ionized donors at RT, resulting in the high electron concentration above $1.0 \times 10^{20} \text{ cm}^{-3}$ at an implant dose of $4.0 \times 10^{15} \text{ cm}^{-2}$, corresponding to P-donor concentration of $2.0 \times 10^{20} \text{ cm}^{-3}$. Based on the Fermi-Dirac distribution, the concentration of ionized donors is calculated to be $1.8 \times 10^{19} \text{ cm}^{-3}$, assuming that the ionization energy of P donors is 45 meV (Ref. 5) and the electron effective mass is $0.39m_0$, where m_0 is the free-electron mass.¹² The calculated activation ratio is only 9%, which is much smaller than the apparent activation ratio of 50% obtained from the Hall effect measurements. Both the decrease of ionization energy for P donors and band gap narrowing due to high donor concentration may explain the

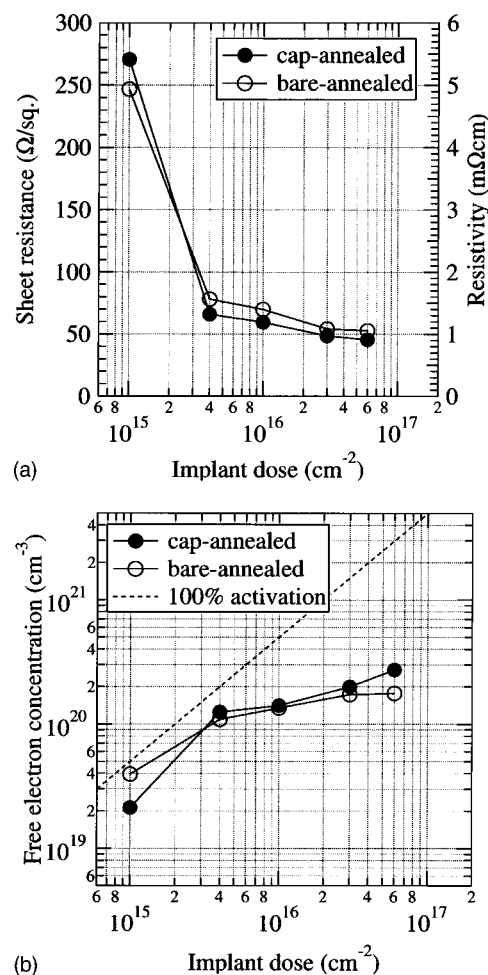


FIG. 4. Implant-dose dependence of (a) sheet resistance (resistivity) and (b) free-electron concentration for high-dose P^+ -implanted 4H-SiC (0001).

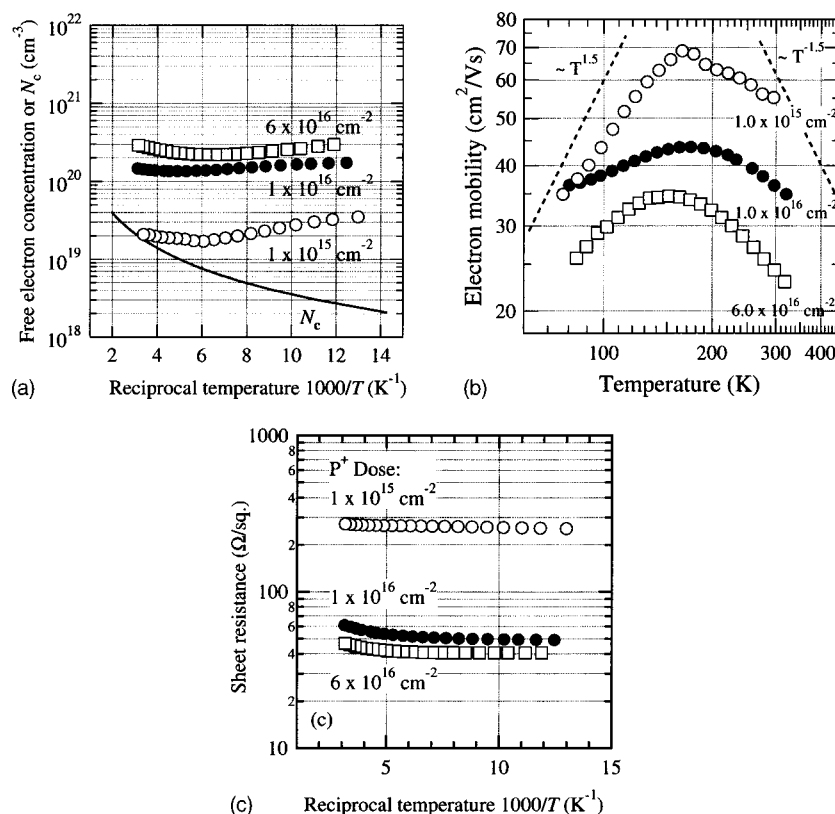


FIG. 5. Temperature dependence of (a) free-electron concentration; (b) electron Hall mobility; and (c) sheet resistance (resistivity) for 4H-SiC (0001) implanted with a P^+ dose of 1.0×10^{15} , 1.0×10^{16} , and $6.0 \times 10^{16} \text{ cm}^{-2}$.

calculated small activation ratio of 9%. At a P-donor concentration of $2 \times 10^{20} \text{ cm}^{-3}$, the ionization energy should be smaller than the value of 45 meV which has been obtained in the donor concentration of the 10^{18} cm^{-3} range.⁵ The band gap narrowing at a high donor concentration may be attributed to the change of lattice parameters.

When the implant dose increases from $4.0 \times 10^{15} \text{ cm}^{-2}$ to $6.0 \times 10^{16} \text{ cm}^{-2}$, the free-electron concentration increases slightly from $1.3 \times 10^{20} \text{ cm}^{-3}$ to $2.7 \times 10^{20} \text{ cm}^{-3}$. The small apparent activation ratios in the high-dose range are attributed partly to higher compensation generated by implantation-induced defects which trap donor electrons. The compensation should increase with the increase of implant dose. The solubility limit of P in SiC may also affect the small apparent activation ratios in the high-dose range. In the literature, the solubility of P has been determined as $2.8 \times 10^{18} \text{ cm}^{-3}$ at 2150°C ,¹⁴ while free-electron concentrations of more than 10^{20} cm^{-3} for P^+ -implanted 4H-SiC have been experimentally shown in the present study and also in a recent report.⁵ These contradict the paper on the solubility of P in SiC.¹³ In fact, the solubility of Al having a similar mass to P is about 10^{21} cm^{-3} at 2400°C .² The solubility of P might be similar to that of Al.

It is important to provide information about annealing temperature at which the graphite cap may no longer be required. In this study, annealing temperature is fixed at 1700°C to investigate the P^+ -dose dependence of electrical properties for 4H-SiC (0001). Recent reports have shown that annealing at 1500°C may bring reasonably low sheet

resistances.^{6,14} The annealing at 1500°C , however, also causes surface roughening due to macrostep formation. The surface morphology of implanted SiC does not depend only on annealing temperature, but on annealing time and implant dose. In the case of bare annealing in an Ar ambient, both sufficient implant activation (low sheet resistance) and good surface morphology could be realized only by the combination of relatively lower implant dose (i.e., $4 \times 10^{15} \text{ cm}^{-2}$) and high-temperature ($\geq 1500^\circ\text{C}$) annealing for a very short time (RTA). The graphite cap is very effective when the implant dose is quite high and/or when high-temperature RTA is not employed.

Figure 5 shows the temperature dependence of (a) free electron concentration; (b) electron Hall mobility; and (c) sheet resistance for samples with a dose of 1.0×10^{15} , 1.0×10^{16} , and $6.0 \times 10^{16} \text{ cm}^{-2}$. All samples were annealed with a graphite cap. The solid curve in Fig. 5(a) depicts the effective density of states in the conduction band (N_c), where N_c is calculated assuming that the electron effective mass is $0.39m_0$. For all the samples, the value of free-electron concentration is larger than N_c as shown in Fig. 5(a). Furthermore, all samples show weak temperature dependences. These results indicate that all these samples are degenerated semiconductors.

The electron Hall mobility is displayed in Fig. 5(b); Mobilities of 55, 35, and $25 \text{ cm}^2/\text{Vs}$ were obtained from the Hall effect measurements at RT for the graphite-cap-annealed samples with a dose of 1.0×10^{15} , 1.0×10^{16} , and $6.0 \times 10^{16} \text{ cm}^{-2}$, respectively. A high-temperature annealing

at 1700 °C brought remarkable lattice recovery of implanted SiC,¹⁴ resulting in the high mobility despite heavy doping. The lower mobility for the $6.0 \times 10^{16} \text{ cm}^{-2}$ -dose sample is attributed to the higher donor concentration and remaining damages induced by implantation. For all samples, the mobility decreases significantly by ionized impurity scattering, as the temperature decreases in the low-temperature range. Although the mobility for the three samples was reduced, the temperature dependence of sheet resistance is very small at lower temperatures as in Fig. 5(c). A quantitative analysis for the temperature dependence of the carrier concentration and mobility requires a theory considering the transport mechanism of electrons in a degenerated semiconductor.

IV. CONCLUSIONS

The authors have investigated high-dose P⁺ implantation followed by high-temperature annealing with a graphite cap. The graphite cap converted from photo-resist suppressed the migration of Si and C atoms on a SiC surface during high-temperature annealing at 1700 °C, resulting in excellent flatness with a roughness of 1.0 nm at a dose of $1.0 \times 10^{16} \text{ cm}^{-2}$. The electrical properties were characterized using Hall effect measurements. No significant difference was observed between graphite-cap-annealed samples and bare-annealed samples. The sheet resistance was significantly reduced down to 70 Ω/□ at a dose of $4.0 \times 10^{15} \text{ cm}^{-2}$. The lowest resistivity of 0.9 mΩcm, corresponding to a sheet resistance of 46 Ω/□, could be achieved by high-dose implantation of $6.0 \times 10^{16} \text{ cm}^{-2}$. The sheet resistance shows a weak temperature dependence.

ACKNOWLEDGMENTS

This work was supported by Grant-in-Aid for JSPS Fellows (for Y. N.), Grant-in-Aid for the 21st Century COE program 14213201, from the Ministry of Education, Culture, Sports, Science and Technology of Japan, and also by TEPCO Research Foundation (for T. K.).

- ¹H. Matsunami and T. Kimoto, *Mater. Sci. Eng., R.* **20**, 125 (1997).
- ²Yu. A. Vodakov and E. N. Mokhov, *Silicon Carbide* 1973 (University of South Carolina Press, Columbia, S. C., 1974), p. 508.
- ³F. Schmid, M. Laube, G. Pensl, G. Wagner, and M. Maier, *J. Appl. Phys.* **91**, 9182 (2002).
- ⁴J. A. Gardner, A. Edwards, M. V. Rao, N. Papanicolaou, G. Kelner, O. W. Holland, M. A. Capano, M. Ghezzi, and J. Kretschmer, *J. Appl. Phys.* **83**, 5118 (1998).
- ⁵M. Laube, F. Schmid, G. Pensl, G. Wagner, M. Linnarsson, and M. Maier, *J. Appl. Phys.* **92**, 549 (2002).
- ⁶M. A. Capano, R. Santhakumar, R. Venugopal, M. R. Melloch, and J. A. Cooper, Jr., *J. Electron. Mater.* **29**, 210 (2000).
- ⁷M. A. Capano, S. Ryu, J. A. Cooper, Jr., M. R. Melloch, K. Rottner, S. Karlsson, N. Nordell, A. Powell, and D. E. Walker, Jr., *J. Electron. Mater.* **28**, 214 (1999).
- ⁸S. E. Sadow, J. Williams, T. Isaacs-Smith, M. A. Capano, J. A. Cooper, Jr., M. S. Mazzola, A. J. Hsieh, and J. B. Casady, *Mater. Sci. Forum* **338–342**, 901 (2000).
- ⁹K. A. Jones, P. B. Shah, K. W. Kirchner, R. T. Lareau, M. C. Wood, M. H. Ervin, R. D. Vispute, R. P. Sharma, T. Venkatesan, and O. W. Holland, *Mater. Sci. Eng., B* **61–62**, 281 (1999).
- ¹⁰J. Senzaki, S. Harada, R. Kosugi, S. Suzuki, K. Fukuda, and K. Arai, *Mater. Sci. Forum* **389–393**, 795 (2002).
- ¹¹H. Nakamura, H. Watanabe, J. Yamazaki, N. Tanaka, and R. K. Malhan, *Mater. Sci. Forum* **389–393**, 807 (2002).
- ¹²W. M. Chen, N. T. Son, C. Persson, U. Lindefelt, O. Kordina, E. Sörman, A. O. Konstantinov, B. Monemar, and E. Janzén, *Phys. Rev. B* **53**, 15409 (1996).
- ¹³Yu. A. Vodakov, E. N. Mokhov, M. G. Ramm, and A. D. Roenkov, *Springer Proc. Phys.* **56**, 329 (1992).
- ¹⁴Y. Negoro, N. Miyamoto, T. Kimoto, and H. Matsunami, *Appl. Phys. Lett.* **80**, 240 (2002).